Journal of Neuroscience Research 79:106–113 (2005)

Evaluation of Brain Mitochondrial Glutamate and α-Ketoglutarate Transport Under Physiologic Conditions

Deborah A. Berkich,[1] Yuping Xu,[1] Kathryn F. LaNoue,[1]* Rolf Gruetter,[2] and Susan M. Hutson[3]

[1]Department of Cellular and Molecular Physiology, Pennsylvania State University, College of Medicine, Hershey, Pennsylvania
[2]Department of Radiology, University of Minnesota, Minneapolis, Minnesota
[3]Department of Biochemistry, Wake Forest University School of Medicine, Winston-Salem, North Carolina

Some models of brain energy metabolism used to interpret in vivo ^{13}C nuclear magnetic resonance spectroscopic data assume that intramitochondrial α-ketoglutarate is in rapid isotopic equilibrium with total brain glutamate, most of which is cytosolic. If so, the kinetics of changes in ^{13}C-glutamate can be used to predict citric acid cycle flux. For this to be a valid assumption, the brain mitochondrial transporters of glutamate and α-ketoglutarate must operate under physiologic conditions at rates much faster than that of the citric acid cycle. To test the assumption, we incubated brain mitochondria under physiologic conditions, metabolizing both pyruvate and glutamate and measured rates of glutamate, aspartate, and α-ketoglutarate transport. Under the conditions employed (66% of maximal O_2 consumption), the rate of synthesis of intramitochondrial α-ketoglutarate was 142 nmol/min·mg and the combined initial rate of α-ketoglutarate plus glutamate efflux from the mitochondria was 95 nmol/min·mg. It thus seems that much of the α-ketoglutarate synthesized within the mitochondria proceeds around the citric acid cycle without equilibrating with cytosolic glutamate. Unless the two pools are in such rapid exchange that they maintain the same percent ^{13}C enrichment at all points, ^{13}C enrichment of glutamate alone cannot be used to determine tricarboxylic acid cycle flux. The α-ketoglutarate pool is far smaller than the glutamate pool and will therefore approach steady state faster than will glutamate at the metabolite transport rates measured.

Key words: brain; α-ketoglutarate; glutamate; mitochondrial metabolite transport; citric acid cycle

A long-standing goal of neurochemists has been to establish noninvasive techniques to monitor O_2 consumption and citric acid cycle flux in the whole brain (Aureli et al., 1997; Dienel and Hertz, 2001; Gruetter et al., 2001). With the advent of functional nuclear magnetic resonance (NMR) imaging of the brain that maps areas activated by specific intellectual tasks, the problem has become even more interesting (Ugurbil et al., 2000; Lee and Chang, 2004). Functional imaging is possible because of local changes in NMR proton relaxation times in activated brain areas (Ogawa et al., 1998). These proton changes may be due to changes in blood flow, increased O_2 uptake, or increased glycolysis, but if O_2 uptake could be monitored specifically in a spatially resolved way, one could test these possibilities. Likewise, if reliable methods for assessing citric acid cycle flux become available, pathologic conditions could be monitored and areas of neurodegeneration identified.

Some years ago an innovative method was proposed for noninvasively measuring brain glucose oxidation and citric acid cycle flux (Sibson et al., 1997). Although this method has been used in a number of studies (Sibson et al., 1998, 2001), it is criticized by others (Gruetter et al., 2001; Henry et al., 2002, 2003; Xu et al., 2004). The technique employs ^{13}C NMR spectroscopy and monitors the carbon 4 of glutamate labeled with ^{13}C as [1-^{13}C]glucose is infused into humans or animals. The 2, 3, and 4 carbons of glutamate can be easily monitored kinetically by ^{13}C NMR spectroscopic techniques. The carbon 4 of glutamate is labeled by [1-^{13}C]glucose in the first turn of the citric acid cycle but not in subsequent turns. The measurement of the kinetics of [4-^{13}C]glutamate appearance in the brain thus provides an unambiguous measure of whole brain glutamate turnover. The assumption is then made that glutamate is in rapid equilibrium with α-ketoglutarate and changes in [4-^{14}C] enrichment in glutamate reflect those in [4-^{13}C]α-ketoglutarate. This assumption is supported by the high

Contract grant sponsor: National Institutes of Health; Contract grant number: NS38641, NS38672.

*Correspondence to: Kathryn F. LaNoue, PhD, Professor, Department of Cellular and Molecular Physiology, Pennsylvania State University, College of Medicine, 500 University Drive, H166, Hershey, PA 17033.
E-mail: klanoue@psu.edu

Received 8 July 2004; Revised 23 August 2004; Accepted 23 August 2004

Published online 22 November 2004 in Wiley InterScience (www.interscience.wiley.com). DOI: 10.1002/jnr.20325

activity of mitochondrial and cytosolic aspartate aminotransferases. A potential flaw in the assumption is that the glutamate monitored is mostly cytosolic whereas the α-ketoglutarate, which reflects flux through the citric acid cycle, is inside the mitochondrial matrix space. Mitochondrial transport of α-ketoglutarate or glutamate (V_x) across the mitochondrial inner membrane would have to be an order of magnitude faster than citric acid cycle flux (V_{TCA}) to validate the assumption that the ^{13}C enrichment in the C-4 of glutamate is always equal to the ^{13}C enrichment of mitochondrial [4-^{13}C]α-ketoglutarate.

Various tests of the hypothesis have involved examination of the kinetics of appearance of ^{13}C in [2,3-^{13}C] of glutamate and of aspartate (Mason et al., 1995; Sibson et al., 1998; Gruetter et al., 2001; Henry et al., 2002). If the assumption is correct, there would have to be a precursor/product relationship between [4-^{13}C]glutamate and [2-^{13}C] glutamate that appears only in the second turn of the cycle. Some of these analyses have supported the hypotheses (Mason et al., 1992, 1995); others have not (Gruetter et al., 2001). Strangely, despite the fairly vigorous controversy, the rate of transport of glutamate and α-ketoglutarate into and out of isolated brain mitochondria has not been monitored under physiologic conditions.

The present study was undertaken to estimate flux through α-ketoglutarate and glutamate transporters while isolated brain mitochondria were oxidizing pyruvate and glutamate under physiologic conditions. We measured citric acid cycle flux directly using measurements of O_2 consumption and rates of pyruvate and glutamate consumption when both were present in the incubation medium.

Transport of α-ketoglutarate and glutamate into and out of the mitochondria was estimated simultaneously. O_2 consumption was set at 66% of its maximal rate. Maximal rates were determined in medium with saturating ADP concentrations (5 mM). Rates of respiration below maximal were established with the aid of a hexokinase/ATP trapping system. The initial concentration of ADP was low (0.1 mM) but the ADP was regenerated with the enzyme hexokinase plus its substrate glucose. Hexokinase phosphorylates glucose to glucose-6-phosphate converting ATP to ADP, and varying hexokinase varies respiration rates. The incubation contained a physiologic concentration of bicarbonate and free Ca^{2+} was buffered at 0.244 μM using an EGTA/Ca^{2+} buffer (Patton et al., 2004). The results of the investigation show that under the conditions used, which were designed to maximize the transport rates, α-ketoglutarate and glutamate transport are of the same order of magnitude as citric acid cycle flux, not an order of magnitude faster as suggested by other workers (Mason et al., 1995). The results are discussed in light of new discoveries about the distribution of the aspartate/glutamate mitochondrial carrier in the brain.

MATERIALS AND METHODS

Isolation of Rat Brain Mitochondria

For isolating brain mitochondria, a modification of the method of Rosenthal et al. (1987) was used, which is one of two methods currently in use. The other method (Clark and Nicklas, 1970) generates synaptosomal-free mitochondria. To isolate synaptosomal-free mitochondria, crude mitochondria are passed through a Ficoll gradient to separate synaptosomes from mitochondria. On the other hand, the method of Rosenthal et al. (1987) breaks the synaptosomal membrane using a low concentration of digitonin, which releases the synaptosomal mitochondria from the synaptosomes. The protease Nagase is also used to break up actin and intermediate filaments.

In our hands, yields from the Rosenthal method (Rosenthal et al., 1987) are about twice as high as that from the Ficoll method (Clark and Nicklas, 1970) (~5–6 mg/rat brain) and the respiratory control ratios are higher as well. The Rosenthal method thus seems to provide a more representative sample of total brain mitochondria (neuronal plus glial).

After anesthetizing 300–400 g male Sprague-Dawley rats, we removed the skull and extracted the whole brain. The cortex was separated from the rest of the brain, minced and washed free of blood with buffer containing 225 mM mannitol, 75 mM sucrose, 5 mM HEPES (pH 7.2), 1 mM EGTA, 1 mg/ml bovine serum albumin (BSA) and then the brain was homogenized in the same buffer with 0.5 mg/ml Nagase added and pH adjusted to 7.3. Homogenate was diluted in buffer containing mannitol, sucrose, and HEPES in the same concentrations as above and mitochondria isolated by differential centrifugation. Digitonin was included in the first high-speed centrifugation but not subsequent ones.

Incubations

Mitochondria were incubated in a buffer containing (in mM): KCl 110; HEPES 20; $MgCl_2$ 5; KH_2PO_4 5; $KHCO_3$ 25; glucose 5; ADP 0.1; $CaCl_2$ 0.6; EGTA 1; glutamate 5; and pyruvate 1. Hexokinase was added to a final concentration of 2 U/ml. The buffer was equilibrated with 95% O_2/5% CO_2 and pH adjusted to 7.3.

Malate concentration was 0.5 or 5 mM. Free Ca^{2+} was set at 0.244 μM using the computer program MaxChelator (Patton et al., 2004) to determine the influence of EGTA/Ca^{2+} ratios on free calcium in our specific medium. Temperature was maintained at 37°C. Ca^{2+} was set at this concentration because α-ketoglutarate dehydrogenase has a k_a for free Ca^{2+} of 0.15 μM (Wan et al., 1989).

Some incubations included [U-^{14}C]glutamate with a specific activity of ~500 dpm/nmol whereas other incubations contained [2-^{14}C]pyruvate at ~3,000 dpm/nmol when measuring ^{14}C-metablites or 500 dpm/nmol when measuring $^{14}CO_2$ production. All incubations included either 5 or 0.5 mM malate.

The reactions were initiated with 0.5–0.8 mg mitochondrial protein. Samples were taken at 0, 2, 4, 6, 8, and 10 min. Protein was precipitated with perchloric acid (final concentration 2%). Total specific activity in the neutralized, protein-free filtrates were determined by scintillation counting. ^{14}C-Metabolites were separated by ion exchange chromatography using Dowex-1 acetate columns as described previously (Gamberino et al., 1997). Mass amounts of α-ketoglutarate, aspartate, glucose-6-phosphate, glutamate, and pyruvate were determined enzymatically (Bergmeyer, 1965; Williamson and Corkey, 1969), and protein was measured using the Bio-Rad reagent.

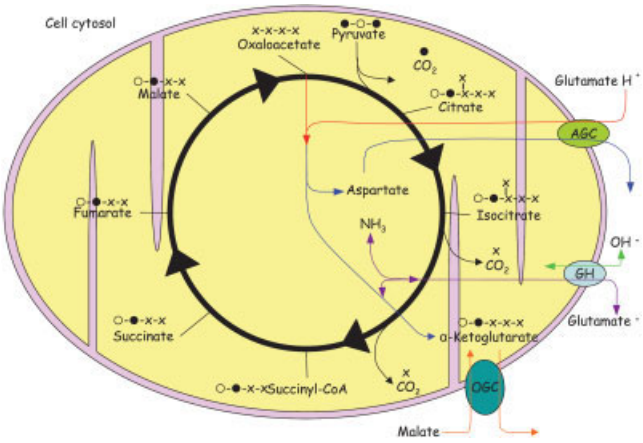

Fig. 1. Citric acid cycle including selected mitochondrial metabolite transporters. Anaplerosis is not included in the diagram. The carbon atoms of citric acid cycle intermediate oxaloacetate are given the symbols X, whereas pyruvate carbons are designated with either filled or open circles. The ^{14}C-labeled carbon in the 2 position of pyruvate is given the open circle. The carbons of the metabolites are shown to retain these symbols as they are metabolized. The transporters are designated OGC for the oxoglutarate carrier (malate/α-ketoglutarate exchanger), GH for the glutamate/hydroxyl carrier, and AGC for the aspartate/glutamate carrier. The diagram illustrates the fact that the labeled carbon [2-^{14}C] of the pyruvate is not lost as $^{14}CO_2$ in the first turn of the citric acid cycle.

When [2-^{14}C]pyruvate was used as the labeled substrate, parallel incubations were run to measure production of $^{14}CO_2$. Mitochondria were added to vials containing 1 ml of medium preequilibrated with 95% O_2/5% CO_2. The vials were sealed with rubber stoppers with a trap (a plastic well containing a fluted square of filter paper) attached. Mitochondria were incubated for 2, 5, or 8 min. At the end of the designated time, 100 μl of 1 N NaOH was injected into the filter paper trap and 100 μl 20% perchloric acid was injected into the incubation medium. The vials were shaken at room temperature for 2 hr and then ^{14}C in the filter paper trap was measured by liquid scintillation counting.

O_2 consumption was measured polarographically at 37°C in separate incubations using a closed vessel with a Clark electrode.

Methods of Calculation

Figure 1 shows the citric acid cycle, highlighting reactions that produce 2 e^-/molecule. The electrons move through the electron transport chain toward cytochrome oxidase, which uses the electrons to reduce oxygen to H_2O. The relevant movements of metabolites (glutamate and α-ketoglutarate) across the mitochondrial membrane are also shown in Figure 1. The α-ketoglutarate carrier catalyzes exchange of malate for α-ketoglutarate. There are two functional glutamate carriers; one catalyzes a unidirectional exchange of protonated glutamate for aspartate and another catalyzes the exchange of glutamate for a hydroxyl ion as illustrated (Palmieri, 2004). The labeled carbon atom of pyruvate is indicated in Figure 1 as an open circle. Figure 1 shows that this carbon will likely be trapped in the large malate pool of the standard media.

Calculations of fluxes through the various steps are made assuming that certain relationships hold. Symbols have the following meaning:

- $\Delta O_2/\Delta t$, rate of O_2 consumption (natoms O/min · mg protein)
- A, pyruvate dehydrogenase flux (nmol pyruvate oxidized/min · mg protein)
- B, isocitrate dehydrogenase flux (nmol isocitrate oxidized/min · mg protein)
- C, α-ketoglutarate dehydrogenase flux (nmol α-ketoglutarate oxidized/min · mg protein)
- D, succinate dehydrogenase flux (nmol succinate oxidized/min · mg protein)
- E, malate dehydrogenase (nmol malate oxidized/min · mg protein)
- $+\Delta$ asp/Δt, rate of appearance of aspartate in the medium
- Δ [U-^{14}C]glu/Δt, rate of disappearance of [U-^{14}C]-glutamate from the medium when [U-^{14}C]glutamate is initial substrate
- $+\Delta\alpha KG/\Delta t$, rate of appearance of α-ketoglutarate in the medium
- $+^{14}$C glu/Δt, rate of appearance of ^{14}C-glutamate in the medium when [2-^{14}C]pyruvate is the initial substrate.

We then assume:

- $\Delta O_2/\Delta t = A + B + C + D + E$,
- A = rate of disappearance of pyruvate mass and ^{14}C in the [2-^{14}C]pyruvate experiments,
- B = A,
- $C = A - \Delta\alpha KG/\Delta t + \Delta[U\text{-}^{14}C]Glu/\Delta t - \Delta^{14}Cglu/\Delta t$ (rate of pyruvate dehydrogenase minus efflux of α-ketoglutarate mass plus the rate of disappearance of [U-^{14}C]glu and minus the efflux of ^{14}C-glutamate when [2-^{14}C]pyruvate is the labeled substrate),
- D = C, and
- E = A + Δasp/Δt (the conversion of malate to oxaloacetate is necessary for transamination of glutamate to aspartate).

One can estimate citric acid cycle flux either by measuring $\Delta O_2/\Delta t$ (oxygen consumption) directly and estimating flux through the individual dehydrogenase reactions, or by measuring each step as described above and comparing the sum of the fluxes generating $2e^-$ with the rate of O_2 consumption. In this study, the two methods agree within about 20%.

The appearance of α-ketoglutarate in the medium is linear for at least 6 min. This initial rate of α-ketoglutarate efflux from the mitochondria provides the value of $\Delta\alpha KG/\Delta t$. The percent changes in glutamate mass were small, but efflux of ^{14}C-glutamate from the mitochondria could be measured in the ^{14}C-pyruvate protocol (Δ^{14}C-glu/Δt) and influx of ^{14}C-glutamate in the ^{14}C-glutamate protocol [U-^{14}C]glu/Δt. From

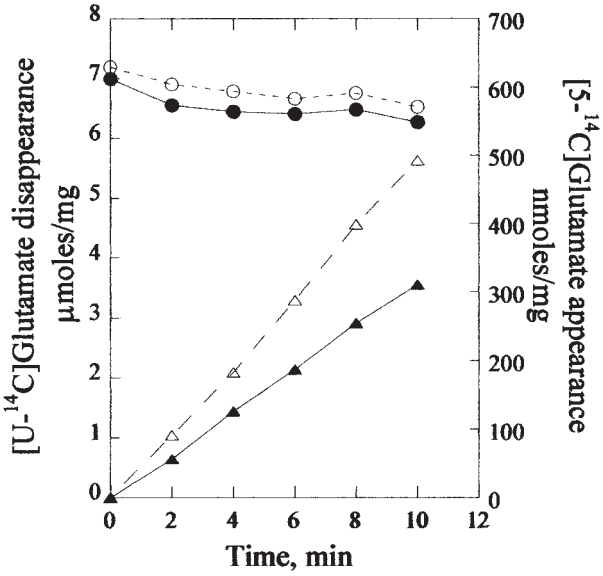

Fig. 2. The influence of time and medium concentrations of malate on ^{14}C-glutamate levels in suspensions of brain mitochondria in physiologic medium. The circles represent [U-^{14}C]glutamate disappearance in medium, which includes 5 mM [U-^{14}C]glutamate and 1 mM (unlabeled) pyruvate. The triangles represent [5-^{14}C]glutamate appearing in medium that includes unlabeled 5 mM glutamate and 1 mM [2-^{14}C]pyruvate. The open symbols represent medium with 0.5 mM malate and closed symbols represent medium with 5 mM malate. As shown, the scales are different for glutamate disappearance (left-hand scale) and appearance (right-hand scale). Values shown are means ± SEM. Data are reported in Table II as rates that were determined by linear regression analysis of the curves shown here.

these data and the necessary calculations it is possible to compare α-ketoglutarate and glutamate transport with citric acid cycle flux.

RESULTS

Glutamate Transport

Glutamate transport (inward) was assessed in the incubations with [U-^{14}C]glutamate. Mass of glutamate in each sample was measured at each time point with 5 or 0.5 mM malate, but the percent disappearance of glutamate mass was too slow to measure accurately. The disappearance of radiolabeled glutamate was measured in those protocols that included [U-^{14}C]glutamate and was rapid enough to obtain an estimate. Moreover, we were able to obtain an estimate of glutamate efflux from the mitochondria when [2-^{14}C]pyruvate was the initial substrate, because the glutamate produced was labeled with ^{14}C. The data are illustrated in Figure 2.

α-Ketoglutarate Transport

The appearance of α-ketoglutarate mass in the medium as a function of time in the various incubations is shown in Figure 3. The initial linearity of the efflux suggests that initial rates represent a unidirectional outward transport process. After 5–6 min, some α-ketoglutarate begins to return to the mitochondrial matrix especially in the incubations with 0.5 mM as opposed to 5 mM malate. There was no statistically significant difference in the appearance of α-ketoglutarate mass comparing protocols that contained [U-^{14}C]glutamate as opposed to [2-^{14}C]-pyruvate.

Efflux rates are faster at higher levels of malate medium because α-ketoglutarate efflux is catalyzed by an exchange carrier that transports α-ketoglutarate in exchange for malate (Palmieri, 2004). We have determined previously that the K_m of malate for the α-ketoglutarate/malate exchange in rat heart mitochondria (LaNoue et al., 1973) is 0.36 ± 0.07 mM.

Citric Acid Cycle Flux

If pyruvate were the only substrate, one could easily calculate citric acid cycle flux from O_2 consumption alone or from the consumption of pyruvate because all electron-producing steps (dehydrogenases) would produce electrons at an equal rate. The presence of glutamate as an additional substrate provides some complications. Oxygen consumption was measured in separate incubations in the presence of 5 or 0.5 mM malate. Because we used a hexokinase trap to set O_2 consumption at an intermediate level, we first determined the rate of O_2 consumption with excess ADP (maximum) and then the rate of O_2 consumption with a limiting amount of hexokinase (2 U/ml).

The O_2 consumption under the experimental conditions used in this study was 66% of maximal (Table I). Rates of O_2 consumption were not affected significantly by the malate concentration used in the incubations. The data used to calculate fluxes through the citric acid cycle are shown in Tables II and III.

Table II provides the ^{14}C data as a function of time. These values were obtained by separating metabolites generated during the incubations by ion exchange chromatography. The Dowex acetate column routinely used in our laboratory (Lieth et al., 2001) separates glutamate, aspartate, and lactate but the citric acid cycle intermediates, citrate, succinate, α-ketoglutarate, fumarate, and malate remain on the column and are not eluted. Before running the columns, the [2-^{14}C]pyruvate in the samples was converted to lactate so that the disappearance of [2-^{14}C]-radiolabeled pyruvate could be followed (Fig 4). Separate experiments were designed to measure $^{14}CO_2$ (Fig 4). Because of the position of the ^{14}C label on the carbon-2 atom of pyruvate, very little accumulated as $^{14}CO_2$. Instead, it was trapped as ^{14}C-malate in the large malate pool (see Fig. 1) after one turn of the cycle.

The data of Table III were obtained by measuring metabolite masses as a function of time. The pyruvate mass and the disappearance of [2-^{14}C]pyruvate provided similar values for pyruvate disappearance. When changes in [U-^{14}C]glutamate were followed, the rate of [U-^{14}C]-glutamate disappearance was found to be faster than that of glutamate mass (Fig. 2). In addition, a very significant rate of appearance of [5-^{14}C]glutamate from [2-^{14}C]pyruvate was measured. Using these data for the appearance and

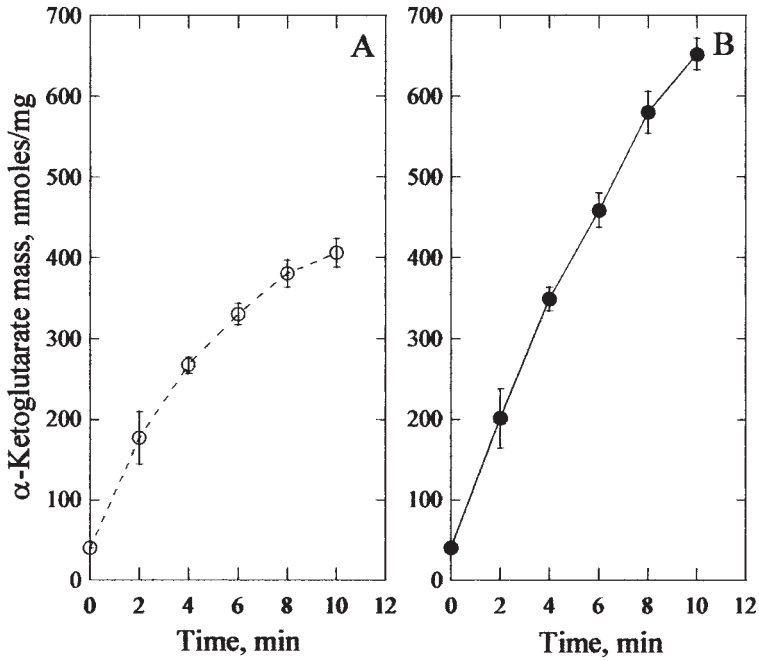

Fig. 3. The influence of time and malate concentration on the appearance of α-ketoglutarate mass in suspensions of brain mitochondria metabolizing glutamate plus pyruvate. **A:** Increases in α-ketoglutarate mass in the presence of 0.5 mM malate. **B:** Increases in α-ketoglutarate mass in the presence of 5 mM malate. Values shown are means ± SEM ($n = 4$). Rates of change are provided in Table III and were obtained by linear regression analysis of the data of Figure 3.

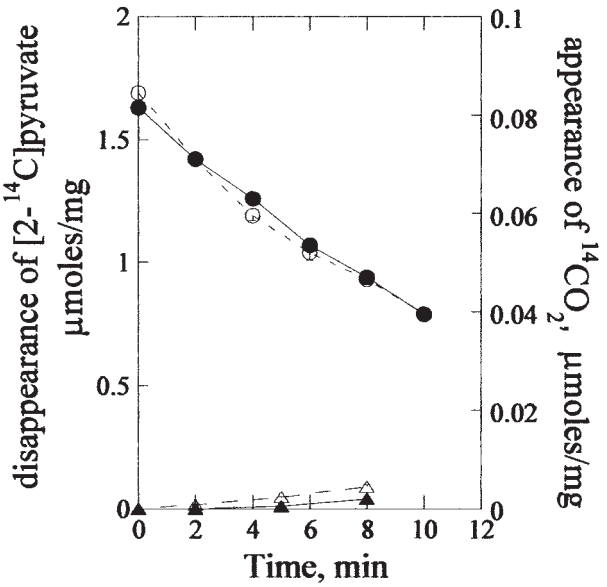

Fig. 4. The influence of time and malate concentration on disappearance of [2-^{14}C]pyruvate and appearance of $^{14}CO_2$ in a suspension of brain mitochondria in physiologic medium. The circles represent [2-^{14}C]pyruvate levels and the triangles $^{14}CO_2$ in medium that initially included 1 mM [2-^{14}C]pyruvate and 5 mM unlabeled glutamate. Open symbols represent medium with 0.5 mM malate and closed symbols represent medium with 5 mM malate. As shown, the scales are different for [2-^{14}C]pyruvate (left-hand scale) and $^{14}CO_2$ (right-hand scale). Rates are reported in Table II and were determined by linear regression analyses.

disappearance of glutamate and the disappearance of [2-^{14}C]pyruvate (Table II and III) it was possible to calculate flux through the different steps of the citric acid cycle as described above. Results of the calculations are provided in Table IV. The dehydrogenase steps are not all equal because of influx of glutamate and malate, as well as initial rates of α-ketoglutarate efflux.

TABLE I. Respiration Rates of Brain Mitochondria*

Conditions	0.5 mM Malate	~5 mM Malate
A	713 ± 35	728 ± 30
B	485 ± 20	464 ± 14

*Values given are *n*atoms O/min · mg mitochondrial protein (means ± SEM). Mitochondria (0.5 mg/ml) were incubated at 37°C in the standard buffer with either (A) 5 mM ADP to maximally stimulate respiration or (B) 2 units of hexokinase with 5 mM glucose to generate ADP at a slow, constant rate.

DISCUSSION

The studies reported provide initial rates of metabolite transport out of the mitochondria. The data therefore cannot be extrapolated directly to the in vivo situation in the intact brain because a steady state is maintained for most metabolites in vivo. In this study, the system approaches a quasi-steady state as α-ketoglutarate efflux decreases after 6–8 min. This is because the increased levels of extramitochondrial α-ketoglutarate stimulate inward transport.

In the intact brain, however, the rate of α-ketoglutarate efflux is probably similar to that observed here, especially at the more physiologic level of malate (0.5 mM). To achieve steady state in the intact brain, some of the cytosolic α-ketoglutarate is transaminated to cytosolic glutamate via the cytosolic aspartate aminotransferase and some is probably transported directly back into mitochondria. In this study, glutamate mass decreased because

TABLE II. Rates of Change of Radiolabeled Metabolites in Incubations of Brain Mitochondria Under Physiologic Conditions With 1 mM Pyruvate and 5 mM Glutamate†

	Initial ^{14}C substrate			
	[2-^{14}C]Pyr		[U-^{14}C]Glu	
Parameter measured	0.5 mM Malate	5 mM Malate	0.5 mM Malate	5 mM Malate
[U-^{14}C]Glu disappearance	—	—	56.2 ± 15	54.6 ± 21
[5-^{14}C]Glu	50.9 ± 0.9★	31.9 ± 1.2	—	—
[2-^{14}C]Pyr disappearance	86.5 ± 4.2	83.0 ± 6.0	—	—
^{14}C-Asp	Negligible	Negligible	Negligible	Negligible

†Values are given as nmol/min · mg protein (mean ± SEM). Individual data points were obtained by dividing the dpm in metabolite peaks by the specific activity of the metabolite or its precursor. Means of rates were obtained by linear regression analysis of individual data points. Glu, glutamate; Pyr, pyruvate; Asp, aspartate.
★$P < 0.001$ significantly different from 5 mM.

TABLE III. Initial Rates of Change in Metabolites in Incubations of Brain Mitochondria Under Physiologic Conditions With 1 mM Pyruvate and 5 mM Glutamate†

Parameter	0.5 mM Malate	5 mM Malate
$\Delta O_2/\Delta t$	485.0 ± 20.0	464.0 ± 14.0
ΔPyruvate	87.1 ± 5.5	60.3 ± 7.8
Δα-Ketoglutarate	43.9 ± 3.4★	67.4 ± 4.9
ΔAspartate	24.8 ± 2.0★	48.7 ± 3.6

†Values shown are means ± SEM ($n = 4$). Details of conditions are described in Methods. Except for $\Delta O_2/\Delta t$, means of rates (nmol/min · mg) were obtained by linear regression analyses of measured metabolite levels at 0, 2, 4, and 6 min.
★$P < 0.001$ significantly different from 5 mM.

TABLE IV. Summary of Calculations of Individual Dehydrogenase Fluxes★

	Rate (nmol/min · mg)	
Dehydrogenase	0.5 mM Malate	5 mM Malate
A. Pyruvate dehydrogenase	86.5	83.0
B. Isocitrate dehydrogenase	86.5	83.0
C. α-Ketoglutarate dehydrogenase	48.1	38.3
D. Succinate dehydrogenase	48.1	38.3
E. Malate dehydrogenase	111.5	131.7

★Values were calculated as described in Methods.

of the absence of cytosolic (medium) transamination; however the glutamate itself can in theory enter and leave the mitochondria. There are two glutamate transporters in brain mitochondria (del Arco and Satrustegui, 1998; Palmieri et al., 2001; Palmieri, 2004). One is the unidirectional aspartate/glutamate carrier that is expressed as two isoforms, only one of which (Aralar1) is expressed abundantly in brain (Palmieri et al., 2001; Palmieri, 2004). Exchange of glutamate for aspartate is stimulated by Ca^{2+} and is electrogenic (del Arco and Satrustegui, 1998; LaNoue et al., 1974; LaNoue and Tischler, 1974). Because it is driven by the mitochondrial electrical potential, it can only proceed in one direction, glutamate in and aspartate out; therefore, without resynthesis from cytosolic α-ketoglutarate, cytosolic glutamate would decline. There is, however, another glutamate transporter in the brain, the glutamate/hydroxyl carrier, and it can run in reverse. Influx on this transporter is required to provide substrate for glutamate dehydrogenase (Fig. 1) and its reversal is probably responsible for the active efflux of glutamate observed in the present experiments and for the very slow decline of glutamate mass.

The data presented indicate that the α-ketoglutarate/malate exchanger and the glutamate/hydroxyl carrier catalyze only a partial isotopic exchange with mitochondrial α-ketoglutarate. To estimate the extent of this exchange, the rate of synthesis of intramitochondrial α-ketoglutarate was compared to the rate that α-ketoglutarate and glutamate are exported from the mitochondria.

We estimate that about 66% of the α-ketoglutarate synthesized is exported. The rate of synthesis of α-ketoglutarate can be estimated as the rate of glutamate entry plus the rate of isocitrate dehydrogenase. At 0.5 mM malate, net glutamate entry is 56 ± 15 nmol/min · mg and isocitrate dehydrogenase flux is 86 ± 4 nmol/min · mg. The sum is 142 nmol/min · mg. That value can be compared to initial rates of efflux of α-ketoglutarate (44 ± 3 nmol/min · mg) plus glutamate (50.9 ± 0.9 nmol/min · mg). The sum is 95 nmol/min · mg or 67% of the rate that α-ketoglutarate is synthesized within the mitochondria. It thus seems that about 33% of the mitochondrial α-ketoglutarate could proceed around the citric acid cycle without equilibrating with cytosolic glutamate. Similar conclusions can be drawn when 5 mM malate is in the medium.

The data indicate that the use of the kinetics of [4-^{14}C]glutamate turnover alone in the in vivo brain to estimate citric acid cycle flux underestimates the value. It is possible, as shown by some authors (Gruetter et al., 2001; Henry et al., 2002), to obtain more accurate values for V_{TCA} by including in the analysis values for glutamate isotopomers generated in the second turn of the citric acid cycle as well as isotopomers of aspartate. Studies similar to those described here have been carried out with rabbit heart mitochondrial (Lewandowski et al., 1997) and directly compared to measurements of citric acid cycle flux

in intact perfused rabbit hearts perfused with ^{13}C substrates (Lewandowski et al., 1997; O'Donnell et al., 1998, 2004; Griffin et al., 2000). Glutamate dehydrogenase and the glutamate/hydroxyl carrier are very active and functionally important in brain (Plaitakis and Zaganas, 2001; Zaganas et al., 2001) but much less active in hearts, making the analysis more complex in the brain than the heart. In the intact hearts, the rates monitored by [4-^{13}C]glutamate correlate directly with expression of the mitochondrial α-ketoglutarate/malate exchanger (Griffin et al., 2000) and do not correlate with citric acid cycle flux (Lewandowski et al., 1997; O'Donnell et al., 1998, 2004). In most ^{13}C NMR spectroscopic studies that focus on energy metabolism, the citric acid cycle flux is abbreviated as V_{TCA} and the metabolite efflux as V_x. The kinetic model used to calculate fluxes in the heart can be verified independently by measuring V_{TCA} (citric acid cycle flux) independently by other techniques (such as O_2 consumption or substrate consumption). The cardiac data suggest that V_x routinely is lower than V_{TCA} (Lewandowski et al., 1997; O'Donnell et al., 1998, 2004; Griffin et al., 2000).

The situation is likely to be somewhat more complicated in the brain because of the higher activity of the glutamate/hydroxyl carrier and the activity of glutamate dehydrogenase. The kinetics of [4-^{13}C]glutamate turnover, however, may provide a useful way to monitor glutamate transport across the mitochondrial membrane and estimate the malate/aspartate shuttle.

The malate/aspartate shuttle is the most active and most commonly used shuttle required to transfer reducing equivalents from the cytosol to the mitochondria (Meijer, 2003). Reducing equivalents (i.e., NADH) are generated in the cytosol by conversion of lactate to pyruvate via cytosolic lactate dehydrogenase, and by conversion of glucose to pyruvate via the glycolytic pathway.

Because NADH is impermeable to the mitochondrial membrane, a metabolite shuttle system is needed to move the electrons from NADH into the mitochondria where oxidative phosphorylation can generate 2.5 molecules of ATP from the energy made available by transfer of these electrons ($2e^-$/molecule NADH) down the electron transfer chain.

The step in the malate/aspartate shuttle that actually moves the electrons into the mitochondria is the exchange of cytosolic malate for mitochondrial α-ketoglutarate. The malate picks up the electrons from NADH via cytosolic malate dehydrogenase. The α-ketoglutarate efflux from mitochondria partially monitored in the intact brain via the appearance of [4-^{13}C]glutamate may thus provide an estimate of the malate/aspartate shuttle.

Because glucose is the major oxidative substrate of the brain whereas hearts instead prefer fatty acids as substrates, it seems that the in vivo [4-^{13}C]glutamate kinetics in the brain may approximate flux through the malate/aspartate cycle, thereby monitoring glucose oxidation. Glucose consumption generates 2 nmol of NADH in the cytosol for each nmol of glucose. In the absence of oxygen or the absence of an NADH shuttle, the product of glucose metabolism is lactic acid; however, it has been made clear recently that not all brain cells have a functional malate/aspartate shuttle (Ramos et al., 2003). Another transporter required for operation of the shuttle is the aspartate/glutamate carrier. A recent careful study of the expression of this carrier in brain (Ramos et al., 2003) indicates that it is not expressed in brain astrocytes. Because astrocytes are known to export lactate as a major product of glucose metabolism (Tsacopoulos and Magistretti, 1996), the absence of an NADH shuttle in these cells perhaps is not surprising. The brain α-ketoglutarate pool is ~0.1% of the brain glutamate pool. The measurements of α-ketoglutarate and glutamate transport made as part of this study indicate that the transporters catalyze fluxes similar to those of the citric acid cycle. If the specific activity of glutamate and α-ketoglutarate change at equal rates, and if the source of label was only pyruvate dehydrogenase, the transporter flux would have to be an order of magnitude faster. This is clearly not the case. However, estimates of V_{TCA} made by perfusing brains with [1-^{13}C]glucose and measuring turnover of [4-^{13}C]glutamate are clearly not wrong by an order of magnitude as judged by comparison with more complete models (Oz et al., 2004).

The reason for this may be that glucose is a major oxidative substrate for the brain and glucose cannot be oxidized without consumption of the cytosolic NADH generated by glycolysis. This consumption involves movement of $2e^-$ from NADH to malate and exchange of intramitochondrial α-ketoglutarate for malate, which is then oxidized by malate dehydrogenase. From Table IV, it is apparent that in our in vitro study malate dehydrogenase flux is faster than αKG dehydrogenase by more than a factor of two. If allowed to proceed to steady state with a complete malate/aspartate cycle supporting glucose oxidation, malate dehydrogenase would proceed at twice the rate of the other citric acid cycle enzymes. Glutamate would exchange with aspartate at the same rate as pyruvate oxidation (from glucose). This would explain why glutamate turnover in the brain provides a good estimate of citric acid cycle flux, but in other organs where citric acid cycle flux is not linked to glucose oxidation glutamate turnover does not provide a reliable estimate.

ACKNOWLEDGMENTS

This work was supported by grants from National Institutes of Health (NS38641 to S.M.H. and K.F.L. and NS38672 to R.G.).

REFERENCES

Aureli T, Di Cocco ME, Calvani M, Conti F. 1997. The entry of [1-13C]glucose into biochemical pathways reveals a complex compartmentation and metabolite trafficking between glia and neurons: a study by 13C-NMR spectroscopy. Brain Res 765:218–227.

Bergmeyer HU. 1965. Methods of enzymatic analysis. New York: Academic Press.

Clark JB, Nicklas WJ. 1970. The metabolism of rat brain mitochondria. Preparation and characterization. J Biol Chem 245:4724–4731.

del Arco A, Satrustegui J. 1998. Molecular cloning of Aralar, a new member of the mitochondrial carrier superfamily that binds calcium and is present in human muscle and brain. J Biol Chem 273:23327–23334.

Dienel GA, Hertz L. 2001. Glucose and lactate metabolism during brain activation. J Neurosci Res 66:824–838.

Gamberino W, Berkich DA, Lynch CJ, Xu B, LaNoue KF. 1997. Role of pyruvate carboxylase in facilitation of synthesis of glutamate and glutamine in cultured astrocytes. J Neurochem 69:2312–2325.

Griffin JL, O'Donnell JM, White LT, Hajjar RJ, Lewandowski ED. 2000. Postnatal expression and activity of the mitochondrial 2-oxoglutarate-malate carrier in intact hearts. Am J Physiol Cell Physiol 279:1704–1709.

Gruetter R, Seaquist ER, Ugurbil K. 2001. A mathematical model of compartmentalized neurotransmitter metabolism in the human brain. Am J Physiol Endocrinol Metab 281:100–112.

Henry PG, Crawford S, Oz G, Ugurbil K, Gruetter R. 2003. Glucose and glial-neuronal metabolism in a-chloralose anesthetized rats measured by in vivo ^{13}C NMR spectroscopy. 11th Scientific Meeting of the International Society for Magnetic Resonance in Medicine. Toronto, ON. p 1967.

Henry PG, Lebon V, Vaufrey F, Brouillet E, Hantraye P, Bloch G. 2002. Decreased TCA cycle rate in the rat brain after acute 3-NP treatment measured by in vivo 1H-[13C] NMR spectroscopy. J Neurochem 82: 857–866.

LaNoue KF, Meijer AJ, Brouwer A. 1974. Evidence for electrogenic aspartate transport in rat liver mitochondria. Arch Biochem Biophys 161:544–550.

LaNoue KF, Tischler ME. 1974. Electrogenic characteristics of the mitochondrial glutamate-aspartate antiporter. J Biol Chem 249:7522–7528.

LaNoue KF, Walajtys EI, Williamson JR. 1973. Regulation of glutamate metabolism and interactions with the citric acid cycle in rat heart mitochondria. J Biol Chem 248:7171–7183.

Lee WT, Chang C. 2004. Magnetic resonance imaging and spectroscopy in assessing 3-nitropropionic acid-induced brain lesions: an animal model of Huntington's disease. Prog Neurobiol 72:87–110.

Lewandowski ED, Yu X, LaNoue KF, White LT, Doumen C, O'Donnell JM. 1997. Altered metabolite exchange between subcellular compartments in intact postischemic rabbit hearts. Circ Res 81:165–175.

Lieth E, LaNoue KF, Berkich DA, Xu B, Ratz M, Taylor C, Hutson SM. 2001. Nitrogen shuttling between neurons and glial cells during glutamate synthesis. J Neurochem 76:1712–1723.

Mason GF, Gruetter R, Rothman DL, Behar KL, Shulman RG, Novotny EJ. 1995. Simultaneous determination of the rates of the TCA cycle, glucose utilization, alpha-ketoglutarate/glutamate exchange, and glutamine synthesis in human brain by NMR. J Cereb Blood Flow Metab 15:12–25.

Mason GF, Rothman DL, Behar KL, Shulman RG. 1992. NMR determination of the TCA cycle rate and alpha-ketoglutarate/glutamate exchange rate in rat brain. J Cereb Blood Flow Metab 12:434–447.

Meijer AJ. 2003. Amino acids as regulators and components of nonproteinogenic pathways. J Nutr 133(Suppl):2057–2062.

O'Donnell JM, Doumen C, LaNoue KF, White LT, Yu X, Alpert NM, Lewandowski ED. 1998. Dehydrogenase regulation of metabolite oxidation and efflux from mitochondria in intact hearts. Am J Physiol 274: 467–476.

O'Donnell JM, Kudej RK, LaNoue KF, Vatner SF, Lewandowski ED. 2004. Limited transfer of cytosolic NADH into mitochondria at high cardiac workload. Am J Physiol Heart Circ Physiol 286:2237–2242.

Ogawa S, Menon RS, Kim SG, Ugurbil K. 1998. On the characteristics of functional magnetic resonance imaging of the brain. Annu Rev Biophys Biomol Struct 27:447–474.

Oz G, Berkich DA, Henry PG, Xu Y, LaNoue KF, Hutson SM, Grueter R. 2004 Neurological metabolism in the awake rat brain: CO_2 fixation increases with brain activity. J Neurosci (in press).

Palmieri F. 2004. The mitochondrial transporter family (SLC25): physiological and pathological implications. Pflugers Arch 447:689–709.

Palmieri L, Pardo B, Lasorsa FM, del Arco A, Kobayashi K, Iijima M, Runswick MJ, Walker JE, Saheki T, Satrustegui J, Palmieri F. 2001. Citrin and aralar1 are Ca(2+)-stimulated aspartate/glutamate transporters in mitochondria. EMBO J 20:5060–5069.

Patton C, Thompson S, Epel D. 2004. Some precautions in using chelators to buffer metals in biological solutions. Cell Calcium 35:427–431.

Plaitakis A, Zaganas I. 2001. Regulation of human glutamate dehydrogenases: implications for glutamate, ammonia and energy metabolism in brain. J Neurosci Res 66:899–908.

Ramos M, del Arco A, Pardo B, Martinez-Serrano A, Martinez-Morales JR, Kobayashi K, Yasuda T, Bogonez E, Bovolenta P, Saheki T, Satrustegui J. 2003. Developmental changes in the Ca2+-regulated mitochondrial aspartate-glutamate carrier aralar1 in brain and prominent expression in the spinal cord. Brain Res Dev Brain Res 143:33–46.

Rosenthal RE, Hamud F, Fiskum G, Varghese PJ, Sharpe S. 1987. Cerebral ischemia and reperfusion: prevention of brain mitochondrial injury by lidoflazine. J Cereb Blood Flow Metab 7:752–758.

Sibson NR, Dhankhar A, Mason GF, Behar KL, Rothman DL, Shulman RG. 1997. In vivo ^{13}C NMR measurements of cerebral glutamine synthesis as evidence for glutamate-glutamine cycling. Proc Natl Acad Sci USA 94:2699–2704.

Sibson NR, Dhankhar A, Mason GF, Rothman DL, Behar KL, Shulman RG. 1998. Stoichiometric coupling of brain glucose metabolism and glutamatergic neuronal activity. Proc Natl Acad Sci USA 95:316–321.

Sibson NR, Mason GF, Shen J, Cline GW, Herskovits AZ, Wall JE, Behar KL, Rothman DL, Shulman RG. 2001. In vivo (13)C NMR measurement of neurotransmitter glutamate cycling, anaplerosis and TCA cycle flux in rat brain during. J Neurochem 76:975–989.

Tsacopoulos M, Magistretti PJ. 1996. Metabolic coupling between glia and neurons. J Neurosci 16:877–885.

Ugurbil K, Adriany G, Andersen P, Chen W, Gruetter R, Hu X, Merkle H, Kim DS, Kim SG, Strupp J, Zhu XH, Ogawa S. 2000. Magnetic resonance studies of brain function and neurochemistry. Annu Rev Biomed Eng 2:633–660.

Wan B, LaNoue KF, Cheung JY, Scaduto RC Jr. 1989. Regulation of citric acid cycle by calcium. J Biol Chem 264:13430–13439.

Williamson JR, Corkey BE. 1969. Assays of intermediates of the citric acid cycle and related compounds by fluorometric enzyme methods. In: Lowenstein JM, editor. Methods of enzymology. New York: Academic Press. p 435–513.

Xu Y, Oz G, LaNoue KF, Keiger CJ, Berkich DA, Gruetter R, Hutson SM. 2004. Whole brain glutamate metabolism evaluated by steady state kinetics using a double isotope procedure, effects of gabapentin. J Neurochem 90:1104–1116.

Zaganas I, Waagepetersen HS, Georgopoulos P, Sonnewald U, Plaitakis A, Schousboe A. 2001. Differential expression of glutamate dehydrogenase in cultured neurons and astrocytes from mouse cerebellum and cerebral cortex. J Neurosci Res 66:909–913.